Radiated emissions from power feeders for electric propulsion in aircraft

Jesper Lansink Rotgerink
Royal Netherlands Aerospace Centre
Marknesse, The Netherlands

***Abstract*—Electric propulsion is a major focal point for aviation industry towards achievement of international sustainability goals. These developments will cause an inevitable increase in on-board power levels, implying higher voltages and currents. One of the various corresponding challenges in electromagnetic compatibility concerns the radiated emissions of power feeders. This paper focusses on the modelling of these emissions from three-phase power feeders by a combination of multiconductor transmission line modelling for determination of the currents in power feeders, and the Hertzian Dipole method to determine the radiated electric fields. Simulations and measurements are performed on the case of a single wire above ground, as well as a three-phase power feeder, resulting in a good match between theory and practice. The obtained simulation methods can also be used in combination with actual currents flowing onto the cabling, obtained either from measurements or simulations, to estimate the total in situ radiated emissions from three-phase power feeders.**

Keywords—electric flight, radiated emissions, power feeders, multiconductor transmission line

I. INTRODUCTION

European regulations, such as Flightpath 2050, require aviation industry to reach a 75% reduction in CO_2 emissions per passenger kilometre and 90% reduction in NO_x emissions [1]. To reach those objectives the entire industry is highly focussed on the various aspects of sustainable aviation. Among those is the realisation of on-board electric propulsion for various aircraft sizes.

The development of such (hybrid) electric aircraft highly increases the power demands on board, which inevitably also implies higher current and voltage levels. These increases will cause severe challenges in electromagnetic compatibility (EMC) as well as thermal challenges. The Horizon 2020 project EASIER (Electric Aircraft System Integration EnableR) is aiming at development of solutions that mitigate these challenges [2].

One of many EMC challenges to be faced, is to limit the radiated emissions from alternate current (AC) power feeders running between power electronics and the motor. In due time, it may be expected that power electronics and electric motors will be more integrated yielding much smaller lengths of AC feeders, but for shorter term electric flight partial AC power distribution is still expected. Due to higher currents, higher voltages and increased switching in the power electronics, a strong increase in high-frequency noise on the power feeders can be expected. Such currents are well-known causes for radiated emissions [3].

Prediction of radiated emissions of power feeders could be done by using the Hertzian Dipole (HD) method in combination with transmission line (TL) theory. In [4] the Hertzian Dipole method is used to predict radiated emissions from a cable above ground. Measured currents at one line end are used in combination with a transmission line model that includes the effects of the line length and terminations at the ends. The resulting currents are transformed to radiated fields by the Hertzian Dipole method. The same methodology, expanded with some analysis of finite ground planes, is used in [5] to simulate radiated emission testing of automotive cables following CISPR25 [6].

This paper uses multiconductor transmission line (MTL) equations to simulate currents in a three-phase power feeder. These currents are used in combination with the HD method to compute the radiated electric fields. The simulations will be performed in a set-up that is representative for the EUROCAE ED-14G [7] radiated emissions set-up. Results of simulations will be compared to measured emissions for both a single wire above ground, as well as a three-phase power feeder above ground. The advantage of using MTL equations is the possibility of excitation by both differential-mode (DM) and common-mode (CM) currents and the analysis how both affect the radiated emissions. Moreover, when the resulting fields are scaled by the input currents, this computation gives a transfer function between currents on the cabling and radiated electric fields. When this transfer function is used in combination with an excitation of the TL model that corresponds to currents resulting from circuit simulations or measurements of the entire powertrain, this will result in the predicted in situ radiated emissions by the cables as part of the entire powertrain.

The following section introduces the MTL and HD methods, after which section III will introduce the measurement set-up used for validation. Section IV will discuss the results of radiated emission simulations and measurements. Finally, section 0 gives conclusions.

II. SIMULATION MODEL

Consider the three-phase power feeder of which the cross section is shown in Fig. 1. Such a power feeder can be considered as a multiconductor transmission line, with in this case three conductors each with a certain height above ground. The currents and voltages in such a transmission line can be solved by solving the MTL equations [8]:

$$\begin{aligned} \frac{d}{dz}\mathbf{V}(z) &= -\mathbf{Z}\mathbf{I}(z) \\ \frac{d}{dz}\mathbf{I}(z) &= -\mathbf{Y}\mathbf{V}(z). \end{aligned} \tag{1}$$

Here $\mathbf{V}$ and $\mathbf{I}$ are in this case 3-dimensional vectors that contain the voltages with respect to ground and currents of each conductor, along the propagation direction z. The per-

The EASIER project has received funding from the European Union's Horizon 2020 research and innovation programme under grant agreement No 875504

978-1-7281-5579-1/20/$31.00 ©2022 IEEE

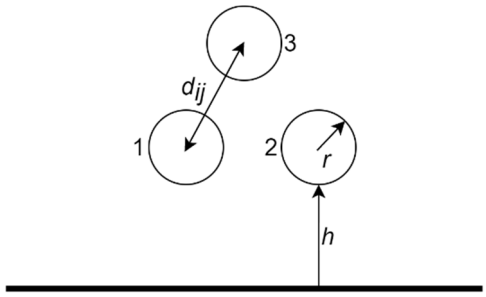

Fig. 1. Cross section sketch of three-phase cable above a ground plane

unit-length (p.u.l.) impedance matrix **Z** and admittance matrix **Y** are given by:

$$\begin{aligned} \mathbf{Z} &= \mathbf{R} + \mathrm{j}\omega\mathbf{L}, \\ \mathbf{Y} &= \mathbf{G} + \mathrm{j}\omega\mathbf{C}, \end{aligned} \tag{2}$$

in which the p.u.l. matrices for resistance **R**, conductance **G**, inductance **L** and capacitance **C** are used. The conductance includes possible losses in surrounding media, which will be neglected in this paper. The resistance matrix can include conductor losses as well as the effects of shielding, such as transfer impedance, in case shielding is applied. Conductor losses for copper wires are small and their effects to radiated emissions of the cabling are small, therefore they are also neglected in the following analysis. Shielding will be considered in follow-up research of this paper and therefore included in possible future publications. However, it will not be considered in this paper.

The inductance and capacitance matrices contain all cross sectional information of the cabling. As shown in Fig. 1 the radius of all three phase conductors equals r and the distance between the phase conductors i and j equals d_{ij}. Together with the height above ground this yields the per-unit-length parameters:

$$\begin{aligned} \mathbf{L} &= \left[l_{ij} \right], \qquad \mathbf{C} = \mu_0 \varepsilon_0 \mathbf{L}^{-1} \\ l_{ii} &= \frac{\mu_0}{2\pi} \ln\left(\frac{2h_i}{r} \right) \\ l_{ij} &= \frac{\mu_0}{4\pi} \ln\left(1 + \frac{4h_i h_j}{d_{ij}^2} \right) \end{aligned} \tag{3}$$

Mind that the heights h_i of each conductor are between centre of the conductor and ground, and can thus be expressed as a combination of the parameters given in in Fig. 1. It is assumed that the relative permittivity and permeability equal one, and thus in (3) only the free space permittivity ε_0 and permeability μ_0 are included. Note that these equations hold for conductors emerged in a homogeneous medium, while the conductors are 'widely' separated. This boils down to the fact that an error of about 2.7% in these values occurs for a ratio of separation/radius equal to 5. Being aware of its limitations, and the fact that there are numerical alternatives for determination of these parameters if effects of insulation and proximity of the conductors should be included, in this section these approximate analytical formulations for inductance and capacitance are applied.

The solution of the MTL equations is obtained by making use of the chain parameter matrix formulations, as in [9]. This requires proper modelling of the terminations of the TL, to act as boundary conditions for the MTL equations. Fig. 2 and Fig. 3 show two terminations schemes, which model either the terminations when the power feeder is contained in a full powertrain or in a measurement set-up. The block in the middle represents the transmission line itself, in which the evolution of voltages and currents over the length of the transmission line is determined by equation (1). In Fig. 2 the terminations include on the left-hand side effects of resistances and capacitances of the LISN as well as an EMI filter. Moreover, on each lead of the power feeder an output filter is included. The load-side represents the behaviour of an electric motor [10]. The source side also contains for each conductor a voltage source. In this way, the terminations are included into the MTL equations by a Thevenin representation:

$$\mathbf{V}_0 = \mathbf{V}_S - \mathbf{Z}_S \mathbf{I}_0, \tag{4}$$

in which $\mathbf{V}_0$ and $\mathbf{I}_0$ are the voltages and currents of each phase conductor at the source side of the transmission line. The voltage sources are contained in the vector $\mathbf{V}_S$, which can either ensure a CM or DM excitation by using equal phase for each conductor, or giving each conductor 120 degrees phase difference. Fig. 3 gives the representation of the terminations in measurements when the cable is excited in common-mode. The 50 Ω represents the internal impedance of the measurement equipment.

Solving a cascaded version of the transmission line equations by using Uniform Cascaded Sections (UCS) yields the currents on all three conductors along the length of the transmission line. These currents can be used as input for the HD method to compute the corresponding radiated electric fields. The vertically polarised field originating from each of these segments can be computed by [4][5]:

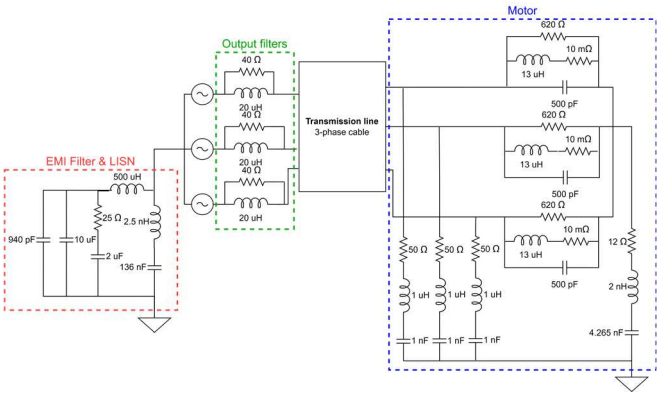

Fig. 2. Terminations of the three-phase transmission line contained in a full powertrain, including at the source side effects of the LISN, EMI filter and output filters, and at the load side the motor.

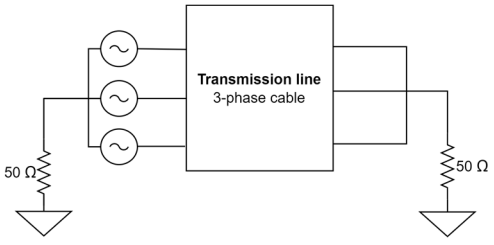

Fig. 3. Terminations of the three-phase transmission line in a measurement set-up.

$$E_v = \frac{I_n \ell z y \eta_0 \beta_0^2}{4\pi r_P^2}\left(\frac{\mathrm{j}}{\beta_0 r_P} + \frac{3}{\beta_0^2 r_P^2} - \frac{3\mathrm{j}}{\beta_0^3 r_P^3}\right)\mathrm{e}^{-\mathrm{j}\beta_0 r_P}. \quad (5)$$

Here the current on each segment is given by I_n, the length of the segment is ℓ, y and z the positions of the observation point respective to the line, β_0 and η_0 the propagation speed and intrinsic impedance and finally r_P the distance from segment to observation point. Summation over all cable segments yields the total electric field at the observation point.

Using the MTL equations provides two ways of applying the HD method, either to each of the separate phase conductors with corresponding currents separately, or to the entire cable at once by using an equivalent CM model with CM currents at the middle of that cable. In both cases, as was also indicated by [4], proper modelling of the terminal currents and their effect on radiated emissions is essential. As in [4] the CM currents to ground are incorporated by including those currents on wire segments running to ground (as well as their counterparts mirrored in the ground plane) in the summation of electric fields originating from all cable segments. This paper focusses on excitation by CM signals, since validation measurements for these are present. For these cases the two models yield exactly the same result, as is shown by Fig. 4, which shows radiated emission of the three-phase power feeders further analysed in section IV, computed in the two different ways indicated above. Future research will also include the analysis of radiated emissions of functional DM currents, including possible effects of imbalances in geometry or terminations. In such cases analysis by computing electric fields from all conductors separately might come in useful, since geometry aspects like loop sizes between phase conductors will become important. The computation of simulated radiated fields in this paper are performed with the single CM current at the centre of the cable.

Since MTL models are at the basis of the presented methods, frequency limitations are determined by the assumptions in transmission line theory.

III. Measurement Set-up

For the purpose of validation, measurements of power feeder emissions were performed. The set-up that was used corresponds with the procedures of EUROCAE ED-14G [7]. In this standard, vertically polarised electric fields are measured and the obtained levels should not exceed given limits for equipment to be compliant. Three pictures of the set-up are shown in Fig. 5, in which radiated emissions of the three-phase power feeder are measured with three different antenna types. The emissions are measured in the frequency range of 10 kHz up to 400 MHz, in which three antennas are used to cover this frequency range:

- Rod antenna: 10 kHz – 30 MHz
- Biconical antenna: 30 MHz – 200 MHz
- Double-ridged horn antenna: 200 MHz – 400 MHz

The only (intentional) deviation in our the test setup when compared to ED-14G is that the rod antenna set-up is extended with a ground plane attached to the metal table (see Fig. 5b). This is done to better compare measurements and simulations, since in this paper the MTL model models an infinite ground plane (when making use of additions given in [5], finite

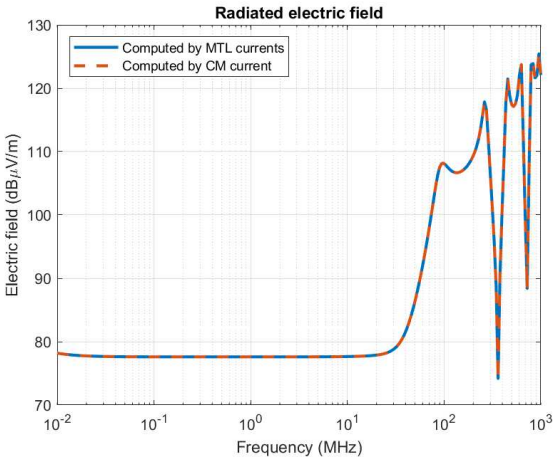

Fig. 4. Comparison of radiated electric field computed with all MTL currents on each of the phase conductors (blue line) and with an equivalent CM current at the central axis of the cable (red dashed line).

Fig. 5. Pictures of the measurement set-up: a) top picture – with horn antenna, b) lower left picture - with the rod antenna, and c) lower right picture - with the double-ridged horn antenna. In all cases a power feeder is placed 10 cm from the edge of a conducting table, and the antenna 90 cm away from the table.

ground planes could also be investigated, but that is not considered in this paper). Moreover, power lines should be of 1 m length in a radiated emissions test. In the presented measurements the single wire is of 1 m length, but after fabrication of the prototypes the three-phase cables turned out to be 87 cm. Apart from that, the position at which the field is measured is consistent with ED-14G and thus always 90 cm next to the table and 30 cm above the table, while the cable is placed horizontally on the table, 10 cm from the edge of the table at a height of 5 cm. For larger three-phase cables these instructions are interpreted as having a block of 5 cm foam below the cabling (e.g. the bottom of the cable is 5 cm above the table, not the centre of the cable), and by placing the closest conductor 10 cm away from the edge of the table.

The measurement set-up is calibrated following ED-14G procedures. In our case the excitation is tuned to be such that the current injected into the cabling is equal to 10 mA. In the

case of the three-phase cable this is CM, so the 10 mA divides over the three phase conductors.

IV. Results

This section describes the results for both simulations and measurements of radiated emissions. Firstly, results of a single wire above ground are discussed. Secondly, the radiated fields of the three-phase cable are evaluated.

A. *Single wire above ground*

Consider a single wire with radius 1.78 mm and 1 m length placed at 5 cm above the ground plane. The wire is terminated on both sides by 50 Ω to ground and excited with 80 dBµA current at the source side over the entire frequency range. The resulting radiated electric field in is shown in Fig. 6. Only the vertically polarized component of the field is shown, since that can be compared to measurements. In Fig. 6 the blue curve is generated by the HD model with the currents obtained from an MTL model, as introduced in section II. For validation purposes, the same case has also been run in Altair Feko [11], shown by the red curve. The results between these two simulations match perfectly. Finally, the yellow curve shows the obtained measured results, which also match very well with simulations. Starting at 10 MHz some fluctuations are superposed onto the general trend of the radiated emissions, which are caused by the measurement set-up. Several experiments on the measurement set-up pointed out that for instance loops generated by the attached table to ground can cause such extra loops.

From the results in Fig. 6 it becomes clear that for low frequencies the radiated emissions are constant. Starting at roughly 10 MHz the emissions start to increase, after which beyond 100 MHz long line resonances can be observed.

B. *Three-phase power feeder*

The next step is to evaluate radiated emissions caused by three-phase power feeders. Fig. 7 shows the results for the radiated electric field originating from a trefoil cable as in Fig. 1, obtained by simulations with the HD+MTL models introduced in section II, simulations with Feko and measurements. For this feeder with a length of 87 cm the wire radius r = 3.67 mm, the height h = 5 cm and the separation d_{ij} = 22.34 mm. The feeder is again excited by a 80 dBµA current, this time applied to the three wires which are tied together. Therefore, the 80 dBµA is distributed over the three phase conductors. The results of the two different simulation methods match very well over the entire frequency region. Moreover, simulation results also match well to the measured radiated emissions. As with the single wire above ground, for low frequencies the radiated emissions are constant, until at roughly 10 MHz they start to increase. Above 100 MHz resonances start to occur due to the cable length, which are well predicted by the simulations. Only extra fluctuations due to the measurement set-up, which were also observed in Fig. 6, cause some deviations between simulations and measurements in the frequency area around 100 MHz.

In the design of AC power feeders for electrically propulsed aircraft there is a clear trade-off between thermal and EMC phenomena. Usually, for EMC, loops are preferred to be small, while thermally it is preferred to separate phase conductors to allow for convective cooling by air. To support such trade-offs the effects of increased separation distances between phase conductors to radiated emission are investigated. Fig. 8 shows the results of simulations and measurements for varying separation distances. In this case, the effects are negligibly small. The main explanation for this is found in the CM excitation. Increasing separation while keeping h fixed to 5 cm ensures that only the loop between the upper conductor in Fig. 1 ground becomes larger, while the

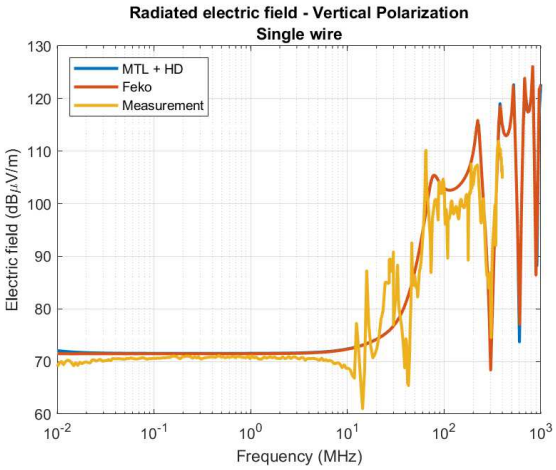

Fig. 6. Simulated and measured radiated electric fields for a single wire above ground. Simulations by the MTL + HD method as introduced in section II (blue) and by Feko (red).

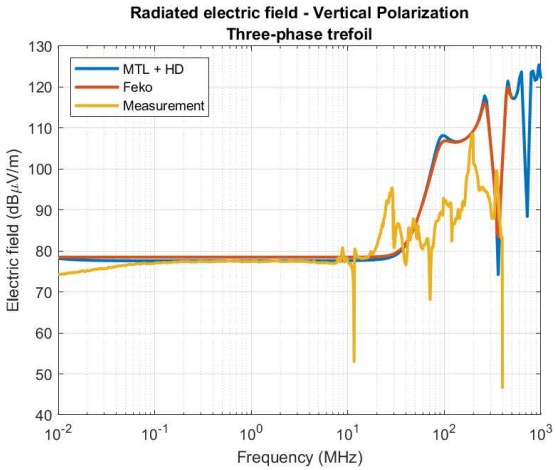

Fig. 7. Simulated and measured radiated electric fields for a three-phase cable above ground. Simulations by the MTL + HD method as introduced in section II (blue) and by Feko (red).

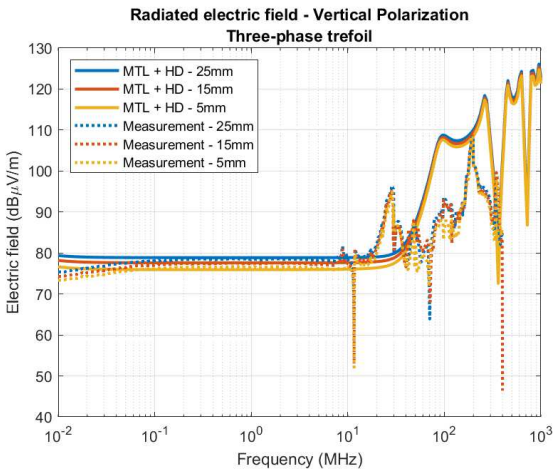

Fig. 8. Simulated (solid lines) and measured (dashed lines) radiated electric fields for a three-phase cable above ground, with varying separations between the phase conductors. Simulation results are obtained by the MTL + HD method as introduced in section II.

other CM loops remain equal in size. It is very likely that the separation affects radiation of functional (DM) currents much more. This will be part of future research and publications.

C. *Total radiation of power chain*

The previous sub-sections showed results of radiation for cables that are excited with a constant current over the entire frequency range, and with loading corresponding to Fig. 3. When these results are scaled to 1 A excitation, they could be considered as a transfer function from cable currents towards radiated emissions. They indicate how much radiated emissions can be expected at each frequency if a cable is excited by one Ampère of current in a specific powertrain. When the loading in RE simulations is changed to reflect those of an actual powertrain, and the obtained results are combined with the actual current running in this powertrain in which the cable is applied, this would result in the total in situ radiated emissions of that power feeder.

To demonstrate this use, consider a three-phase cable inserted into an electric propulsion powertrain shown in Fig. 9. This is a powertrain which includes LISN, EMI filter, a two-level DC-AC converter (inverter), output filters on the converter side of the cables, and an electric motor. These components are also represented by the terminations in Fig. 2. Simulated results of the currents that can be expected in such a powertrain are obtained by a Matlab Simscape model of this powertrain (details not shown in this paper). The CM component of that current flowing into a single phase conductor as part of a three-phase cable is shown by the red curve in Fig. 10. In the same figure, the radiated electric field from that same three-phase cable with loads corresponding to this powertrain (i.e. loads in Fig. 2) are shown. In this case, excitations are scaled such that 1 A CM current flows on each of the three phase conductors, hence the units (dBµV/mA). When compared to the results in Fig. 7 these simulated radiated emissions contain some extra resonances in the lower frequency area that are caused by the behaviour of the termination schematics.

Since the radiated field is scaled to 1A CM current, the two results in Fig. 10 can be combined by multiplication to obtain the total radiation of the power feeders in this power train. These in situ simulated radiated emissions in the frequency domain are shown in Fig. 11. This figure also shows two examples of radiated emission limits given by EUROCAE ED-14G section 21 [7]. Two limits for two different categories are shown, where the applicable category depends on for instance the location in the aircraft and the distance to sensitive on-board radio equipment. Category B in this case is the one with least restrictions to radiated emissions, while category H has much higher restrictions. Limits for radiated emissions are shown only for 100 MHz upwards, since most recent versions of ED-14 do not require testing for lower frequencies. Nevertheless, simulation results are also shown for lower frequencies, mainly out of research interest. Moreover, certain airframers such as Airbus still require to do testing in accordance with older ED-14 versions that still require testing for lower frequencies (including for instance 150 kHz – 30 MHz).

The result in Fig. 11 shows that the expected radiated emissions for this power feeder can be large. In the area above 100 MHz several peaks exceed even the most relaxed emission limit for category B, and the results will certainly not pass the testing for category H. This shows the need for EMI mitigations in the powertrain for electric propulsion, which is

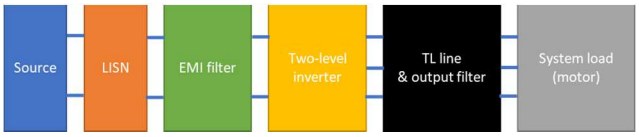

Fig. 9. Currents flowing onto the power cable for a power train including a two-level inverter.

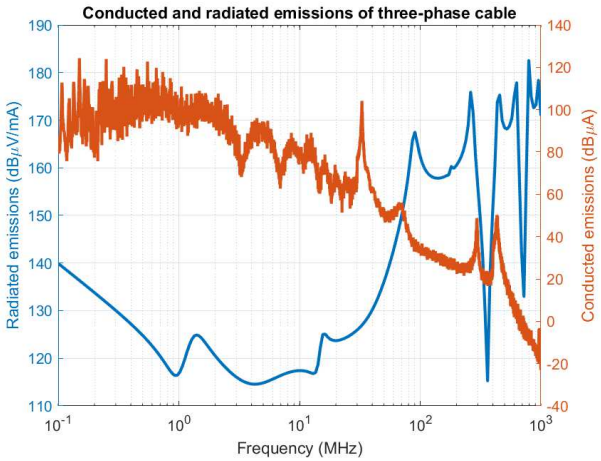

Fig. 10. Simulated radiated emissions when the cable with loading equal to those in Fig. 2 is excited by a 1 A CM current (blue), and simulated CM currents flowing onto the power cable situated in a power train schematically given by Fig. 9 (red, obtained by Matlab Simscape).

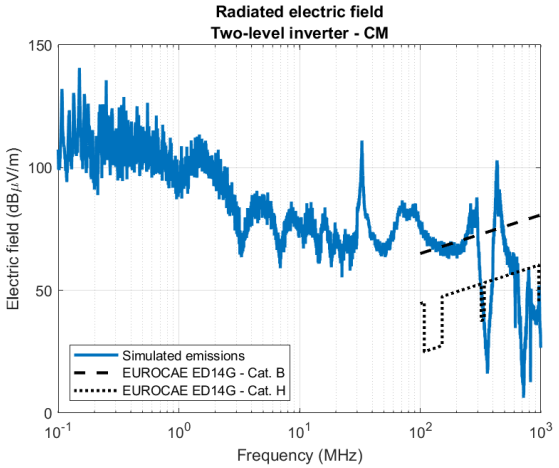

Fig. 11. Simulated total in-situ radiated electric field for a three-phase power feeder in a power-train like the one illustrated in Fig. 9.

one of the major topics for EASIER research. Several improved power feeders have been defined that include EMI mitigation techniques, mainly focussed on providing a return path for the CM current inside the power feeder to decrease CM loop areas. These are in the process of testing and results will be included in future publications. Moreover, on the power electronics side of things, various improvements are researched, among which optimized EMI filters and modulation schemes to suppress high frequency noise.

V. Conclusions

This paper presents a way to predict by simulation the radiated emissions generated by power feeders in a powertrain on-board aircraft with electric propulsion. Multiconductor transmission line simulations are combined with the Hertzian Dipole method to convert currents on the conductors of power feeders to radiated electric fields. Results of simulation and

measurement are compared for both the case of a single wire above a ground plane, and a three-phase power feeder above ground. Simulated results by the MTL+HD method are also compared to Feko simulations. In general, results between the two simulation methods match perfectly, and also the match with measurements is very good. Variations in separation between phase conductors are shown to be negligibly small for the CM excitations used in this paper.

The models introduced in this paper can also be used to excite the cabling with actual expected currents in a complete powertrain, including for instance power converters, EMI filters and electric motor. Such currents can be either obtained by measurements, or for instance Simscape modelling. In this paper, this is illustrated by computing the in-situ radiated emissions caused by cabling in a realistic powertrain for electric propulsion. This yields the observation that the expected radiated emissions could be large when compared to limits given in standards such as ED-14G. This indicates the need for research into EMI mitigation solutions for such powertrains. This is part of the research within the EASIER project in which the addressed research has been carried out. Future publications should describe further the effects of these mitigation solutions.

ACKNOWLEDGMENT

Thanks to our partners in the EASIER consortium for all useful feedback and data in the modelling process for this paper. Specifically thanks to project partners from Collins Aerospace Applied Research and Technology in Ireland for providing Simscape models that were used in the final part of this paper, and to GKN Fokker Elmo for providing test samples of power feeders used for measurements.

REFERENCES

[1] European Commission, “Flightpath 2050: Europe’s vision for aviation,” LU: Publications office, 2011

[2] https://www.easier-h2020.eu/

[3] C.R. Paul, “Introduction to electromagnetic compatibility,” Hoboken NJ, USA: Wiley, 2006.

[4] J. Meng, Y.X. Teo, D.W.P. Thomas, C. Christopoulos, “Fast prediction of transmission line radiated emissions using the Hertzian dipole method and line-end discontinuity methods,” IEEE Trans. On Electromagn. Compat., vol. 56, no. 6, Dec. 2014

[5] J. Jia, D. Rinas, S. Frei, “Predicting the radiated emissions of automotive systems according to CISPR 25 using current scan methods,” IEEE Trans. On Electromagn. Compat., vol. 58, no. 2, April 2016.

[6] “CISPR 25: Vehicles, boats and internal combustion engines-radio disturbance characteristics – limits and methods of measurements for the protection of on-board receivers,” IEC, third ed., 2008.

[7] European Organization for Civil Aviation Equipment (EUROCAE), “ED 14, Revision G – Environmental conditions and test procedures for airborne equipment,” January 2015.

[8] C.R. Paul, “Analysis of multiconductor transmission lines,” New York, NY, USA: Wiley, 1994.

[9] J. Lansink Rotgerink, H. Schippers and F. Leferink, “Low-frequency analysis of multiconductor transmission lines for crosstalk design rules,” IEEE Trans. On Electromagn. Compat., vol. 51, no. 5, pp. 1612-1620, Oct. 2019.

[10] J. Lee, J. Ha, M. Kim, S. Yun, Y. Kim and W. Nah, “Prediction of Conducted Emission in a PMSM-Drive Braking System Using a Circuit Model Combined with EM Simulation,” Intern. Journal of Automotive Techn., vol. 20, pp. 487-498, May 2019.

[11] Altair Feko – http://www.altairhyperworks.com/product/feko